New azaspiracid analogues detected as bi-charged ions in Azadinium poporum (Amphidomataceae, Dinophyceae) isolated from Japanese coastal waters

New azaspiracid analogues detected as bi-charged ions in *Azadinium poporum* (Amphidomataceae, Dinophyceae) isolated from Japanese coastal waters

Mayu Ozawa[a], Hajime Uchida[a], Ryuichi Watanabe[a], Satoshi Numano[a], Ryoji Matsushima[a], Hiroshi Oikawa[a], Kazuya Takahashi[b], Wai Mun Lum[b], Garry Benico[c], Mitsunori Iwataki[b], Toshiyuki Suzuki[a]*

[a] *Fisheries Technology Institute, Japan Fisheries Research and Education Agency, 2-12-4 Fukuura, Kanazawa, Yokohama, Kanagawa 236-8648, Japan*

[b] *Graduate School of Agricultural and Life Sciences, The University of Tokyo, 1-1-1 Yayoi, Bunkyo, Tokyo 113-8657, Japan*

[c] *Department of Biological Sciences, Central Luzon State University, Science City of Muñoz, Nueva Ecija, Philippines*

E-mail address: ozawa_mayu81@fra.go.jp (M. Ozawa), uchida_hajime03@fra.go.jp (H. Uchida), watanabe_ryuichi73@fra.go.jp (R. Watanabe), numano_satoshi55@fra.go.jp (S. Numano), matsushima_ryoji60@fra.go.jp (M. Matsushima), oikawa_hiroshi04@fra.go.jp (H. Oikawa), kazuyat-dino@g.ecc.u-tokyo.ac.jp (K. Takahashi), lum_wai_mun00@fra.go.jp (W.M. Lum), gabenico@clsu.edu.ph (G. Benico), iwataki@g.ecc.u-tokyo.ac.jp (M. Iwataki),

suzuki_toshiyuki@fra.go.jp (T. Suzuki)

* Corresponding author

Highlights

・Japanese *Azadinium poporum* produces AZA2 as dominant toxin and several AZAs.

・Twelve new AZAs were discovered from Japanese *Azadinium poporum*.

・New AZAs detected as bi-charged ions were discovered.

・AZAs detected as bi-charged ions were sulfated AZAs and some had hexoses.

Keywords

Azadinium poporum, azaspiracids, LC-MS/MS, bi-charged ion, hexose

Abbreviations

AZA, azaspiracid; LC-MS/MS, liquid chromatography-tandem mass spectrometry; SRM, selected reaction monitoring; LC-QTOFMS, liquid chromatography-quadrupole time of flight mass spectrometry.

Abstract

Lipophilic marine biotoxin azaspiracids (AZAs) are produced by dinoflagellates *Azadinium* and *Amphidoma*. Recently, several strains of *Azadinium poporum* were isolated from Japanese coastal waters, and detailed toxin profiles of two strains (mdd421 and HM536) among them were clarified by several detection techniques on liquid chromatography-tandem mass spectrometry (LC-MS/MS) and liquid chromatography-quadrupole time of flight mass spectrometry (LC-QTOFMS). In our present study, AZA analogues in seven strains of *A. poporum* from Japanese coastal waters (including two previously reported strains) were determined by these detection techniques. The dominant AZA in the seven strains was AZA2 accompanied by small amounts of several known AZAs and twelve new AZA analogues. Eight of the twelve new AZA analogues discovered in our present study were detected as bi-charged ions on the positive mode LC/MS/MS. This is the first report describing AZA analogues detected as bi-charged ions with hexose and sulfate groups in their structures.

1. Introduction

Azaspiracids (AZAs) are lipophilic polyether compounds with a cyclic amine, a tri-spiro ring, azaspiro ring and a terminal carboxylic acid group [1] (Fig. 1). The first azaspiracid shellfish poisoning, which is characterized by gastrointestinal symptoms including nausea, vomiting, severe diarrhea, and stomach cramps, occurred by

58 consumption of blue mussels (*Mytilus edulis*) cultivated in Ireland (Killary Harbour)
59 [2]. AZA1, 2, and 3 are regulated by several countries including the European Union
60 (EU), at a level of 160 μg AZA1 equivalents kg^{-1} edible shellfish meat [3].
61 *Azadinium spinosum*, *A. poporum*, *A. dexteroporum* and *Amphidoma languida*
62 were identified as the causative species producing AZAs implicated in AZA
63 poisoning cases [4–7]. Bivalve contamination cases exceeding the regulatory level of
64 AZAs and human poisoning cases by consumption of bivalves contaminated with
65 AZAs have not been reported in Japan. Recently we isolated *A. poporum* of ribotype
66 A2, B and C1 producing AZA2 from Japanese coastal waters and clarified detailed
67 toxin profiles of two *A. poporum* strains (mdd421 and HM536) of ribotype C1 [8, 9].
68 More than sixty AZAs have been reported from toxic dinoflagellates and bivalves.
69 These AZAs generally have structurally different functional groups located at C3
70 (R1), C8 (R2), C22 (R3) and C23 (R4) in Fig. 1. The structures of eighteen AZAs
71 were unambiguously elucidated using nuclear magnetic resonance (NMR) technique
72 [1, 10–20] (Fig. 1), while the structures of other AZAs have tentatively identified by
73 tandem mass spectrometric (MS/MS) fragmentation experiment.
74 In our previous study of two strains (mdd421 and HM536) of *A. poporum* isolated
75 from Japanese coastal waters, we reported the discovery of thirteen new AZAs and a
76 complexity of toxic profiles elucidated by a combination of several LC-MS/MS and
77 LC-QTOFMS methods [9]. In the present study, we have clarified toxin profiles of

five additional strains (MoAz592, MoAz593, MoAz594, TOY121 and LAM125) of *A. poporum* isolated from Japanese coastal waters. In addition to four new AZAs, eight new AZAs detected as the bi-charged ions were also discovered in seven strains of Japanese *A. poporum*.

2. Materials and methods

2.1. Chemicals

Certified reference materials (CRMs) of AZA1, 2 and 3 were purchased from the National Research Council (NRC, Ottawa, Canada), and each CRM solution was diluted to 100-fold with methanol and equally mixed. LC/MS grade acetonitrile and analytical grade acetone were purchased from Kanto Chemical Co., Inc. (Tokyo, Japan). Analytical grade formic acid and sodium formate were purchased from FUJIFILM Wako Pure Chemical Corporation (Osaka, Japan). Analytical grade ammonium formate was purchased from and Nacalai Tesque, Inc. (Kyoto, Japan). Distilled and deionized water was passed through a Milli-Q Reference system (Merck, Darmstadt, Germany) to obtain ultrapure purified water with a specific resistance of 18.2 MΩ cm and a TOC of 3 ppb or less.

2.2. Culture of *Azadinium poporum* strains

Five strains of *A. poporum* (MoAz592, MoAz593, MoAz594, TOY121 and

98 LAM125) were isolated from Mutsu Bay and Funka Bay in Japan [8] and these
99 strains were analyzed for comprehensive survey of AZAs for the first time. The algae
100 were grown in 50 mL flasks contained 25 mL f/2-medium under the same cultivation
101 conditions as in our previous study [9]. Cells were harvested by centrifugation in 50
102 mL centrifugation tubes at 600 × *g* for 3 min, and the pellets were stored at –20 °C
103 until analyzed by LC-MS/MS and LC-QTOFMS.
104
105 2.3. Extraction of AZAs from *Azadinium poporum* strains
106 Extraction of AZAs from cell pellets was carried out according to the previous
107 study [9]. Cell pellets were thawed, and 0.4 mL acetone was added to the pellets, then
108 sonicated for 5 min and centrifuged at 1600 × *g* for 5 min to obtain supernatants. The
109 residues were re-extracted with 0.4 mL acetone. The supernatants were combined and
110 transferred to 1 mL measuring flask and made up to 1 mL with acetone. The acetone
111 solutions were centrifuged at 7000 × *g* for 3 min, and the supernatants were
112 transferred into autosampler vials for LC-MS/MS or LC-QTOFMS. Extracts of two
113 *A. poporum* strains (mdd421 and HM536) reported in our previous study [9] were
114 reanalyzed to investigate high molecular weight AZA analogues found from five
115 newly analyzed strains.
116
117 2.4. Analyses

2.4.1. Liquid chromatography-Mass spectrometry

System #1 (LC-MS/MS)

The analytical system #1 consisted of an QTRAP4500 (SCIEX, Framingham, USA), triple quadrupole mass spectrometer with a high-performance liquid chromatograph of Nexera LC-20 series (Shimadzu, Kyoto, Japan). Analysis software was Analyst 1.6.2 (SCIEX, Framingham, USA).

System #2 (LC-QTOFMS)

The analytical system #2 consisted of an micrOTOF-QII (Bruker, MA, USA), quadrupole time-of-fight mass spectrometer (QTOFMS) with high-performance liquid chromatograph of UltiMate 3000 Series (Thermo Fisher Scientific, MA, USA). Analysis software was Data Analysis Version 4.0 SP5.

The chromatographic separation was carried out with two different columns: a C8 column (100 mm × 2.1 mm, 1.9 μm Thermo Hypersil Gold; Thermo Fisher Scientific, Waltham, MA, USA) and a core shell column (100 mm × 2.1 mm, 2.7 μm CAPCELL CORE ADME; Osaka Soda, Osaka, Japan) as reported in our previous study [9]. The mobile phase, flow rate and gradient conditions were also the same as those described in our previous study [9].

2.4.2. Selected reaction monitoring (SRM) analysis

SRM analysis for known AZAs was performed using System #1. SRM ion channels in positive ion mode are shown in Table 1. The following MS parameters were applied: curtain gas: 15 psi, ion transfer voltage: 4750 V, temperature: 600 ºC, ion source gas 1: 30 psi, ion source gas 2: 60 psi, collision gas: 11 psi, declustering potential (DP): 100 V, entrance potential (EP): 11 V, collision cell exit potential (CXP): 16 V, and collision energies were set the optimal value for each AZA.

2.4.3. Precursor ion scan analysis and neutral loss scan analysis

Precursor ion scan analysis and neutral loss scan analysis were performed on the system #1 scanning between *m/z* 700.0 to *m/z* 900.0 and between *m/z* 900.0 to *m/z* 1100.0 for *m/z* 362.3, 348.3, 364.3, 378.3 and ions losing neutral ions of 54.0 *m/z* units (3 H_2O loss), respectively, as reported in our previous study [9].

2.4.4. Enhanced product ion scan analysis

MS/MS product ion spectra of AZAs detected by SRM, precursor ion scan and neutral loss scan analyses were obtained using positive ion mode enhanced product ion scan analysis. Enhanced product ion scan analysis was carried out on the system #1. The following parameters were applied: curtain gas: 20 psi, ion spray voltage: 5500 V, temperature: 350 °C, ion source gas 1: 50 psi, ion source gas 2: 80 psi,

collision gas: high, DP: 100 V, entrance potential (EP): 10 V, collision energy (CE): 67 V, as reported in our previous study [9].

2.4.5. Quadrupole time of flight mass spectrometric (QTOFMS) analysis

Positive ion mode and negative ion mode survey scan analyses were performed to obtain accurate mass of $[M+H]^+$ and $[M–H]^–$ as reported in our previous study [9].

The elemental composition for $[M+H]^+$ with sufficient intensity were estimated from the accurate mass. MS/MS analysis as performed to obtain MS/MS spectra and to calculate the measured accurate mass and elemental composition of MS/MS product ions was carried out. These various mode analyses were performed using System #2, and ESI conditions were as shown in Table S1.

3. Results and discussion

Several LC-MS/MS and LC-QTOFMS techniques were performed to search for AZA analogues in seven strains of *A. poporum* isolated from the coastal waters of Japan. AZAs detected in the seven strains of *A. poporum* are shown in Table 2.

3.1. Known AZAs

The most dominant AZA detected in the seven strains of *A. poporum* was AZA2. In addition to AZA2, small quantities of several AZA analogues were also detected in

the seven strains (Table 2). Detailed MS/MS product ions, retention times and elemental compositions of compounds 1, 7, 8, 9, 12 and 17 were reported in our previous study [9], where these compounds were identified as putative AZA analogues.

3.2. New AZAs

We identified twelve potential new AZA analogues in the seven strains of *A. poporum*. Detailed information regarding the MS/MS product ions, retention times, and elemental compositions of these new AZA analogues is provided in Table 2. Elemental compositions of the key MS/MS product ions obtained by MS/MS analysis using LC-QTOFMS are also presented in Table 3. Due to high molecular weights and complexity, we were unable to obtain elemental compositions for compounds 23–30. Detailed structural analyses of compounds identified as new AZA analogues are described as follows:

3.2.1. Mono-charged AZAs

Compound 19

Compound 19 exhibited an $[M+H]^+$ ion of *m/z* 800.5 and had an elemental composition of $C_{45}H_{69}NO_{11}$ (Tables 2 and 3). Fig. 3B shows the MS/MS spectrum of compound 19. The MS/MS product ions originating from groups 2 to 5 (*m/z* 644.4,

198 434.3, 334.3, 234.2) were all 28 *m/z* units lower than those of AZA2 (Fig. 3A, Table
199 3). This mass shift indicates that compound 19 has a structure involving the loss of
200 2C4H between C28 and C40 positions in comparison to AZA2. Compound 19 also
201 has a structure involving the loss of CO between C1 and C9. This is the first report of
202 ions with *m/z* 644.4, 434.3, 334.3 and 234.2 being detected as the key products
203 derived from groups 2 to 5 of AZA analogues (Fig. 2)
204
205 Compound 20
206 Compound 20 exhibited an $[M+H]^+$ ion of *m/z* 816.5 and had an elemental
207 composition of $C_{45}H_{69}NO_{12}$ (Tables 2 and 3). The primary MS/MS product ions
208 resulting from cleavages of groups 2 to 5 (*m/z* 672.4, 462.3, 362.3, 262.2) were
209 identical to those obtained for AZA2 (Fig. 3C, Table 3). These MS/MS product ions
210 and elemental composition suggest that compound 20 has a structure involving loss
211 of 3C4H between C1 and C9 positions when compared to AZA2. The major MS/MS
212 product ions and $[M+H]^+$ were consistent with those obtained for AZA34 [15].
213 However, a distinctive MS/MS product ion at *m/z* 772.4 shifted from $[M+H]^+$ by 44
214 *m/z* units losing CO_2 was detected in compound 20 (Fig. 3C) whereas this
215 characteristic ion was not observed in AZA34 [15]. Such a mass shift is observed
216 when hydroxy group is attached to the C3 position of AZAs [18, 21, 22]. This mass
217 shift can be observed when C2–C3 is connected with a double bond. Therefore, it is

218 expected that the structure of compound 20 is AZA34 analogue with the A ring
219 opened structures (Fig. S1 b or c). It was revealed to be a different carbon backbone
220 in comparison with that of AZA34.
221
222 Compounds 21 and 22
223 Compounds 21 and 22 exhibited an $[M+H]^+$ ion of *m/z* 860.5 with an elemental
224 composition of $C_{46}H_{69}NO_{14}$ (Tables 2 and 3). These compounds generated identical
225 MS/MS spectra (Fig. 3D). The product ions deriving from groups 3 to 5 (*m/z* 434.3,
226 334.3, 234.2) were all 28 *m/z* units lower than those of AZA2, and these were
227 consistent with AZA19. The product ion of group 2 (*m/z* 660.4) was 12 *m/z* units
228 lower than that of AZA2. These observations suggest that compounds 21 and 22
229 possess a structure in which 2C4H are removed from positions C28–C40 and an
230 additional oxygen atom is incorporated at positions C10–C19 in comparison with
231 AZA2. Compounds 21 and 22 were identified AZA2–2C4H+2O. Because it is
232 suggested that AZA can be assembled and cyclized from the cyclic amine end [15],
233 there is few possibilities of forming 4 rings by losing 2C4H from 6 rings of the I ring.
234 The loss of 2C4H in the I ring is presumed to be the loss of the methyl groups at C37
235 and C39. Although 39-demethyl AZAs have been reported [16, 20], this is the first
236 report of two-carbon unit smaller AZA such as compounds 19, 21, and 22. It is also
237 suggested that compounds 21 and 22 possess another oxygen atom between positions

238 C2 and C9 when compared to AZA2. The characteristic ion at *m/z* 816.5 shifted from
239 $[M+H]^+$ by 44 *m/z* units was detected (Fig. 3D). This mass shift is observed in 3-
240 hydroxy AZAs such as AZA4, 7, 9, 36, 37 and 48 [18, 21, 22], suggesting the
241 addition of another oxygen atom at C3.
242
243 3.2.2. Bi-charged AZAs
244 In the precursor ion scan analysis of the seven strains, bi-charged ions associated
245 with compounds 23 through 30 were detected. These compounds exhibited
246 characteristic bi-charged ions in both LC/MS/MS and LC/QTOFMS (middle row of
247 Fig. 4A–F). In positive and negative ion modes, molecular related ions corresponding
248 to $[M+H]^+$, $[M+NH_4]^+$, $[M–H]^–$ were detected. Besides these molecular related ions,
249 several bi-charged ions such as $[M+2H]^{2+}$ were identified, providing the molecular
250 weights of bi-charged AZAs. The key MS spectra obtained from the bi-charged AZAs
251 detected on the positive ion mode were assigned as shown in Table 3.
252
253 Compounds 23 and 28
254 Compounds 23 and 28 were exclusively detected from strain mdd421 (Table 2).
255 The MS spectra on positive ion mode LC-QTOFMS analysis appeared somewhat
256 complex, while the MS spectra in negative ion mode were simpler, with the $[M–H]^–$
257 of compound 23 assigned to *m/z* 1484.6016 (Fig. 4A). Therefore, $[M+H]^+$ and

258 $[M+2H]^{2+}$ of compound 23 was assigned as *m/z* 1486.6387 and *m/z* 743.8396,
259 respectively (Fig. 4A, Table 2). Similarly, compound 28 produced comparable ions,
260 with the $[M–H]^{–}$ at *m/z* 1564.5366, and $[M+H]^{+}$ and $[M+2H]^{2+}$ assigned as *m/z*
261 1566.5994 and *m/z* 783.8141, respectively (Fig. 4B, Table 2).
262 For compound 23, a series of ions at *m/z* 1468.6, 1388.6 and 1308.6 were
263 detected, each losing 80 *m/z* units from $[M–H_2O+H]^{+}$ (Fig. 5A). These 80 *m/z* units
264 mass shifts corresponded to loses of HPO_3 or SO_3. Table 4 shows measured accurate
265 mass differences between ions losing 80 *m/z* units for compounds 23–25, 28, 29, 30
266 and AZA2 phosphate ester. We have previously reported the detection of AZA2
267 phosphate in mdd421 and HM536 strains [9]. The average values of two mass shifts
268 of 80 *m/z* units for compound 23 ware 79.9590 (n=3) and 79.9493 (n=3), respectively
269 (Table 4). Theoretical values of calculated exact mass differences due to de-
270 phosphate group ($–HPO_3$) and de-sulfate group ($–SO_3$) are 79.965782 and 79.956266,
271 respectively. In case of AZA2 phosphate ester, mass shifts shown in Table 4 are
272 closer to the theoretical value of $–HPO_3$. In contrast, both mass shifts of compound
273 23 are closer to the theoretical value of $–SO_3$, suggesting that the compound 23 is a
274 sulfated AZA. MS/MS spectra at collision energy (CE) 30 eV for compound 28
275 comprised a series of ions at *m/z* 1548.6, 1468.6, 1388.6 and 1308.8. Each product
276 ion was also shifted by 80 *m/z* units (Fig. 5B). Three mass shifts of 80 *m/z* units on
277 compound 28 were quite close to the theoretical value of $–SO_3$ than $–HPO_3$ (Table 4).

These findings suggest that compounds 23 and 28 have two and three adjacent sulfate groups, respectively, and compound 23 could be the de-sulfated analogue of compound 28.

In MS/MS spectra targeting $[M+H]^+$ of compounds 23 and 28 with a high CE at 100 eV, two mass shifts of 162 *m/z* units were observed from the ion at *m/z* 1308.6 (Fig. 5A and B). The structure corresponding to mass shift of 162 *m/z* units can be attributed to dehydrated hexose [23]. Therefore compounds 23 and 28 are suggested to possess two consecutive hexoses. Furthermore, in MS/MS analyses targeting $[M–H_2O+2H]^{2+}$ of the compounds 23 and 28, characteristic product ions at *m/z* 672.4, 462.3, 362.3 and 262.2 derived from groups 2 to 5 were observed (Fig. 5A and B). These results suggest that compounds 23 and 28 are tri-sulfated-di-hexosyl-AZA and di-sulfated-di-hexosyl-AZA, respectively. It is also suggested that two sugers combined with two or three sulfates could be esterified between C1 and C9 of the AZA basic backbone. These AZA analogues esterified with sulfated glucosides have never been detected in algae and shellfish.

Compound 24

Compound 24 was detected in strains MoAz592, MoAz593 and TOY121 (Table 2). MS spectra in negative ion mode survey scan showed ion at *m/z* 1490.6769 as the $[M–H]^-$, and consequently ions of *m/z* 1492.7023 and *m/z* 746.8483 were assigned

298 $[M+H]^+$ and $[M+2H]^{2+}$ (Fig. 4C). MS/MS spectrum of compound 24 revealed two
299 losses of 80 *m/z* units and one loss of 162 *m/z* units (Fig. 5C).
300 The average values of two mass shifts of 79.9556 (n=3) and 79.9586 (n=3) were
301 close to the theoretical value of de-sulfate group (Table 4). Characteristic ions at *m/z*
302 672.4, 462.3, 362.3 and 262.2 derived from cleavage of groups 2 to 5 were detected,
303 and these product ions matched those obtained for AZA2 (Table 3, Fig. 5C).
304 Therefore, compound 24 was presumed to be di-sulfated-hexosyl-AZA.
305
306 Compounds 25, 26 and 27
307 In the precursor ion scan analysis of strains mdd421 and HM536, compounds
308 25–27 were detected at *m/z* 744.9 ($[M–2H_2O+2H]^{2+}$), and they exhibited the same
309 MS spectra with different retention times (Table 2). Since the negative ion mode
310 showed $[M–H]^–$ at *m/z* 1522.7424, $[M+H]^+$ and $[M+2H]^{2+}$ of compound 27 were
311 presumed to be *m/z* 1524.7818 and *m/z* 762.9090, respectively (Fig. 4D). The MS/MS
312 spectra showed a single mass shift of 80 *m/z* units, with no subsequent loss of 80 *m/z*
313 units or loss of 162 *m/z* units (Fig. 5D). The average values of mass shifts of 79.9507
314 (n=3) obtained for compound 25 were closer to the theoretical value of a de-sulfate
315 group (Table 4). Characteristic ions derived from groups 2 to 5 were the same as
316 those detected in AZA2, indicating that compounds 25 to 27 are AZA analogues with
317 an additional large structure including a sulfate group on the carboxy side chain (Fig.

318 5D). Compound 27 was dominant compared to the other compounds 25 and 26,
319 which were suggested to be isomers of compound 27 (Table 2).
320
321 Compounds 29 and 30
322 Compound 29 was detected in strain MoAz594 (Table 2), and a negative ion
323 mode survey scan showed $[M–H]^–$ at *m/z* 1606.7492 (Fig. 4E). Consequently, MS
324 spectra in positive mode were assigned, and ions at *m/z* 1608.7762 and *m/z* 804.9045
325 detected from compound 29 were assigned to be $[M+H]^+$ and $[M+2H]^{2+}$, respectively.
326 Compound 30 was detected in strains MoAz592 and LAM125 (Table 2). A negative
327 ion mode analysis exhibited $[M–H]^–$ at *m/z* 1754.8104 (Fig. 4F). Consequently, ions
328 at *m/z* 1756.8423 and *m/z* 878.9321 were assigned to be $[M+H]^+$ and $[M+2H]^{2+}$,
329 respectively (Fig. 4F, Table 2). In the MS/MS spectra of compounds 29 and 30, one
330 mass shift of 80 *m/z* units from $[M+H]^+$, followed by one mass shift of 162 *m/z* units
331 and product ions at *m/z* 672.4, 462.3, 362.3 and 262.2 derived from group 2 to 5 were
332 detected (Fig. 5E and F). The average error values of mass shifts, 79.9544 (n=3) and
333 79.9523, were closer to the theoretical value of a de-sulfate group (Table 4). These
334 results suggest that compounds 29 and 30 are sulfated-hexosyl-AZAs with different
335 aglycones.
336 Furthermore, the structure outside of the hexoses or sulfate groups and AZA
337 basic backbone were underdetermined because of the little information of MS/MS

338 fragmentation at *m/z* 800-1000 of compounds 23-30. Except for compounds 23 and
339 28, which were detected in the same strain, there are no compounds with aglycones in
340 common.

341 The relative retention times (RRTs) of each compound for AZA2 are shown in
342 Table 2. The RRTs of sulfated AZAs were lower than That of AZA2. In strain
343 mdd421, the RRT of compound 28 (three sulfate AZA) was lower than that of
344 compound 23 (two sulfate AZA). These results can be explained by more polarity due
345 to sulfated moieties. These data on the RRTs support sulfation on AZA molecular.
346

347 3.3. Toxin profiles in *A. poporum* strains in Japan

348 The extracted LC-QTOFMS chromatograms of AZA2, four new AZAs detected
349 as mono-charged ions, and eight new AZAs detected as bi-charged ions for each *A.*
350 *poporum* strain are shown in Fig. 6. The peak area percentages of AZAs determined
351 by both LC-MS/MS SRM analysis and QTOFMS survey scan analysis were fairly
352 consistent, except for compounds 23–30, which ionized as bi-charged ions (Table 5).
353 The inconsistency in the data for bi-charged ions could be attributed to the
354 complexities of their chemical structures and the complicated MS/MS parameters of
355 SRM MS/MS analysis.

356 The five new strains of ribotype A2 and the two previously isolated strains of
357 ribotype C1 produced AZA2 as the dominant toxin, which is consistent with the

358 results of the previous report [8]. Most of the analogues other than AZA2 were
359 present in trace amounts (Fig. 6, Table 5).
360 The comprehensive survey of AZAs produced by several strains of *A. poporum*
361 revealed that the toxin profiles varied from strain to strain. *A. poporum* culture strains
362 of ribotype A2 and C1 isolated from the Japanese coast commonly produce AZA2
363 and compound 1 [9]. Regardless of genotype, *A. poporum* producing AZA2 contained
364 compound 1 in common, suggesting that the compound 1 is presumably an
365 intermediate in biosynthesis of AZAs. It seems likely that differences in genotypes do
366 not lead to significant differences in AZA toxin profiles in our present study.
367
368 **4. Conclusions**
369 Twelve new putative AZA analogues were discovered in seven *A. poporum*
370 strains isolated from Japanese coastal waters. It is noteworthy that toxic strain
371 primarily produces diverse minor AZAs in addition to the dominant AZA2. It is
372 noteworthy that the first discovery of a new AZA group with loss of 2C4H in the I
373 ring compared to standard AZAs. This is the first discovery of hexosyl AZAs and
374 AZAs with sulfate groups. AZAs detected with bi-charged ions were found in *A.*
375 *poporum* culture strains of ribotype A2 as well as ribotype C1.
376 Our study demonstrated that a combination of several detection modes of LC-
377 MS/MS and LC-QTOFMS in positive and negative modes is invaluable for

identifying new AZA analogues and elucidating the structures of AZA with unique and complex chemical structures. Although the twelve compounds discovered in this study clearly have the basic structure of AZA, further structural elucidation using NMR spectroscopy will be required. Additionally, investigating the intracellular roles and toxicities of AZAs with sulfate group or hexose will be future research objectives.

Credit authorship contribution statement

K.T., W.M.L., G.B. and M.I. performed isolation and identification of *Azadinium* strains. M.O. maintained *Azadinium* culture strains. M.O. and H.U. performed sample analysis by LC-MS/MS etc. S.N., R.W., R.M., H.O. and T.S. contributed on experimental design, providing several assistances in laboratory facilities for instrumental analyses. M.O., H.U. and T.S. performed data evaluation, important discussion as well as experimental design. M.O. and T.S. performed paper writing. H.O. and R.M. contributed on funding. First draft was written by M.O. and T.S., and the review and editing of the draft was performed by all authors.

Declaration of competing interest

The authors declare no conflict of interest.

Acknowledgements

This work was partially supported by the research project on Regulatory research projects for food safety, animal health and plant protection (JPJ008617, 18064849) funded by the Ministry of Agriculture, Forestry and Fisheries of Japan, and JSPS KAKENHI 19KK0160 and 22H02416 (MI).

References

[1] M. Satake, K. Ofuji, H. Naoki, K.J. James, A. Furey, T. McMahon, J. Silke, T. Yasumoto, Azaspiracis, a new marine toxin having unique spiro ring assemblies, isolated from Irish mussels, J. Am. Chem. Soc. 120 (1998) 9967–9968, https://doi.org/10.1021/ja981413r.

[2] T. McMahon, J. Silke, West coast of Ireland: winter toxicity of unknown aetiology in mussles, Harmful Algae News 14 (1996) 2.

[3] Marine biotoxins in shellfish-Azaspiracid group-Scientific Opinion of the Panel on Contaminants in the Food chain, EFSA J. 723 (2008) 1–52, https://doi.org/10.2903/j.efsa.2008.723.

[4] U. Tillmann, M. Elbrächter, B. Krock, U. John, A. Cembella, *Azadinium spinosum* gen. et sp. Nov. (Dinophyceae) identified as a primary producer of azaspiracid toxins, Eur. J. Phycol. 44 (2009) 63–79, https://doi.org/10.1080/09670260802578534.

[5] U. Tillmann, M. Elbrächter, U. John, B. Krock, A new non-toxic species in the dinoflagellate genus *Azadinium*:*A. poporum* sp. Nov., Eur. J. Phycol. 46(1) (2011) 74–87, https://doi.org/10.1080/09670262.2011.556753.

[6] U. Tillmann, R. Salas, M. Gottschling, B. Krock, D. O'Driscoll, M. Elbrachter, *Amphidoma languida* sp. Nov. (Dinophyceae) reveals a close relationship between *Amphidoma* and *Azadinium*, Protist 163 (2012), 701–719, https://doi.org/10.1016/j.protis.2011.10.005.

[7] I. Percopo, R. Siano, R. Rossi, V. Soprano, D. Sarno, A. Zingone, A new potentially toxic *Azadinium* species (Dinophyceae) from the Mediterranean Sea, *A. dexteroporum* sp. Nov., J. Phycol. 49 (2013) 950–966, https://doi.org/10.1111/jpy.12104.

[8] K. Takahashi, G. Benico, W.M. Lum, H. Uchida, M. Ozawa, H. Oikawa, T. Suzuki, N.V. Nguyen, D.V. Ha, M. Iwataki, Toxigenic strains of *Azadinium poporum* (Amphidomataceae, Dinophyceae) from Japan and Vietnam, with first reports of *A. poporum* (ribotype A) and *A. trinitatum* in Asian Pacific, Phycol. Res. 69(3) (2021) 175–187, https://doi.org/10.1111/pre.12455.

[9] M. Ozawa, H. Uchida, R. Watanabe, R. Matsushima, H. Oikawa, K. Takahashi, M. Iwataki, T. Suzuki, Complex profiles of azaspiracid analogues in two culture strains of *Azadinium poporum* (Amphidomataceae, Dinophyceae) isolated from

Japanese coastal waters determined by LC-MS/MS, Toxicon 199 (2021) 145–155, https://doi.org/10.1016/j.toxicon.2021.06.010.

[10] K. Ofuji, M. Satake, T. McMahon, J. Silke, K.J. James, H. Naoki, Y. Oshima, T. Yasumoto, Two analogs of azaspiracid isolated from mussels, *Mytilus edulis*, involved in human intoxication in Ireland, Nat. Toxins 7 (1999) 99–102.

[11] K. Ofuji, M. Satake, T. McMahon, K.J. James, H. Naoki, Y. Oshima, T. Yasumoto, Structures of azaspiracid analogs, azaspiracid-4 and azaspiracid-5, causative toxins of azaspiracid poisoning in Europe, Biosci. Biotechnol. Biochem. 65 (2001) 740–742, https://doi.org/10.1271/bbb.65.740.

[12] K.C. Nicolaou, T.V. Koftis, S. Vyskocil, G. Petrovic, W. Tang, M.O. Frederick, D.Y.K. Chen, Y. Li, T. Ling, Y.M.A, Yamada, Total synthesis and structural elucidation of azaspiracid-1. Final assignment and total synthesis of the correct structure of azaspiracid-1, J. Am. Chem. Soc. 128 (2006) 2859–2872.

[13] K.C. Nicolaou, M.O. Frederick, G. Petrovic, K.P. Cole, E.Z. Loizidou, Total synthesis and confirmation of the revised structures of azaspiracid-2 and azaspiracid-3, Angew. Chem. 45 (2006) 2609–2615.

[14] J. Kilcoyne, A. Keogh, G. Clancy, P. LeBlanc, I. Burton, M.A. Quilliam, P. Hess, C.O. Miles, Improved isolation procedure for azaspiracids from shellfish, structural elucidation of azaspiracid-6, and stability studies, J. Agric. Food Chem. 60 (2012) 2447–2455, https://doi.org/10.1021/jf2048788.

[15] J. Kilcoyne, C. Nulty, T. Jauffrais, P. McCarron, F. Herve, B. Foley, F. Rise, S. Crain, A.L. Wilkins, M.J. Twiner, P. Hess, C.O. Miles, Isolation, structure elucidation, relative LC-MS response, and in vitro toxicity of azaspiracids from the dinoflagellate *Azadinium spinosum*. J. Nat. Prod. 77 (2014) 2465–2474, https://doi.org/10.1021/np500555k.

[16] B. Krock, U. Tillmann, E. Potvin, H.J. Jeong, W. Drebing, J. Kilcoyne, A. Al-Jorani, M.J. Twiner, Q. Gothel, M. Kock, Structure elucidation and in vitro toxicity of new azaspiracids isolated from the marine dinoflagellate *Azadinium poporum*, Mar. Drugs 13 (2015) 6687–6702, https://doi.org/10.3390/md13116687.

[17] J. Kilcoyne, M.J. Twiner, P. McCarron, S. Crain, S.D. Giddings, B. Foley, F. Rise, P. Hess, A.L. Wilkins, C.O. Miles, Structure elucidation, relative LC-MS response and in vitro toxicity of azaspiracids 7–10 isolated from mussels (*Mytilus*

edulis), J. Agric. Food Chem. 63 (2015) 5083–5091, https://doi.org/10.1021/acs.jafc.5b01320.

[18] J. Kilcoyne, P. McCarron, M.J. Twiner, F. Rise, P. Hess, A.L. Wilkins, C.O. Miles, Identification of 21,22-dehydroazaspiracids in mussels (*Mytilus edulis*) and in vitro toxicity of azaspiracid-26, J. Nat. Prod. 81 (2018) 885–893, https://doi.org/10.1021/acs.jnatprod.7b00973.

[19] J. Tebben, C. Zurhelle, A. Tubaro, I. A. Samdal, B. Krock, J. Kilcoyne, S. Sosa, V. L. Trainer, J. R. Deeds, U. Tillmann, Structure and toxicity of AZA-59, an azaspiracid shellfish poisoning toxin produced by *Azadinium poporum* (Dinophyceae). Harmful Algae 124 (2023) 102388, https://doi.org/10.1016/j.hal.2023.

[20] R. Salas, E. Murph, R. Doohan, U. Tillmann, O.P. Thomas, Production of the dinoflagellate *Amphidoma languida* in a large scale photobioreactor and structure elucidation of its main metabolite AZA-39. Harmful Algae 127 (2023) 102471, https://doi.org/10.1016/j.hal.2023.102471.

[21] K.J. James, M. Diaz Sierra, A. Furey, M. Lehane, A. Braña Magdalena,

Detection of five new hydroxyl analogues of azaspiracids in shellfish using multiple tandem mass spectrometry, Toxicon 41 (2003) 277–283, https://doi.org/10.1016/S0041–0101(02)00288–X.

[22] B. Krock, U. Tillmann, D. Voss, B.P. Koch, R. Salas, M. Witt, E. Potvin, H.J. Jeong, New azaspiracids in Amphidomataceae (Dinophyceae), Toxicon 60 (2012) 830–839, https://doi.org/10.1016/j.toxicon.2012.05.007.

[23] H.S. Gadgil, P.V. Bondarenko, M.J. Treuheit, D. Ren, Screening and sequencing of glycated proteins by neutral loss scan LC/MS/MS method, Anal.Chem. 79 (2007) 5991–5999, https://doi.org/10.1021/ac070619k.

517 **Figure legends**

518 **Fig. 1.** Chemical structure of AZA1, 2, 3, 4 and 5.

519

520 **Fig. 2.** The fragmentation diagram of AZAs by positive ion mode LC/MS/MS.

521 *Characteristic product ions in AZA2

522

523 **Fig. 3.** Enhanced product ion LC-MS/MS spectra obtained for culture strains of *A.*

524 *poporum*. (A) AZA2, (B) compound 19, (C) compound 20 and (D) compounds 21

525 and 22.

526

527 **Fig. 4.** MS spectra obtained for culture strains of *A. poporum* by positive ion mode

528 and negative ion mode LC/QTOFMS. (A) compound 23, (B) compound 28, (C)

529 compound 24, (D) compound 27, (E) compound 29 and (F) compound 30.

530

531 **Fig. 5**. MS/MS spectra obtained for culture strains of *A. poporum*. (A) compound 23,

532 (B) compound 28, (C) compound 24, (D) compound 27, (E) compound 29 and (F)

533 compound 30. Target ions and collision energies for MS/MS analyses are shown in

534 each MS/MS spectra.

535

536 **Fig. 6.** Extracted ion chromatograms of AZA1, 2, 3 standard mixture and new AZAs

in *A. poporum* strains on the LC-QTOFMS with a C8 column. (A) AZA1, 2, 3 standard mixture, (B) strain MoAz592, (C) strain MoAz593, (D) strain MoAz594, (E) strain LAM125, (F) strain TOY121, (G) strain mdd421 and (H) strain HM536.

Table legends

Table 1 SRM ion channels of AZAs including new AZA analogues detected in our present study.

Table 2 The measured accurate mass of $[M+H]^+$, elemental compositions, and retention times obtained for AZA analogues using LC-QTOFMS.

Table 3 Elemental compositions of key MS/MS product ions detected from *A. poporum* strains by LC/QTOFMS.

Table 4 The measured accurate mass differences of product ions detected by MS/MS analysis using LC-QTOFMS.

Table 5 The peak area percentages of AZAs in *A. poporum* strains obtained by LC-MS/MS SRM analysis and LC-QTOFMS survey scan analysis.

Supplement

Table S1 ESI conditions of various analysis mode by LC-QTOMS.

Fig. S1 (a) The chemical structures of AZA34 [15] and (b, c) the two putative structures of compound 20.

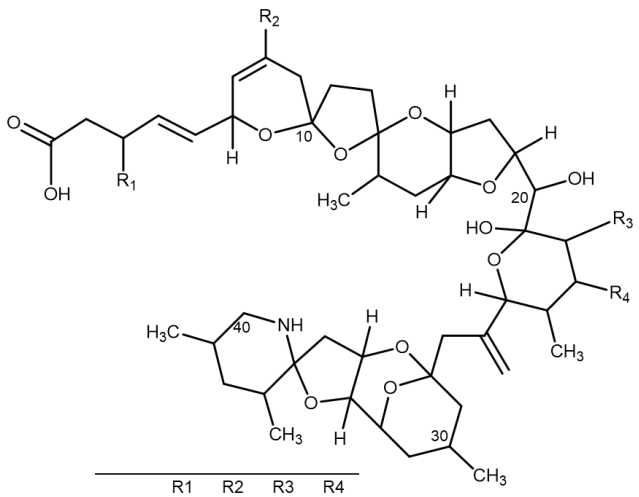

	R1	R2	R3	R4
AZA1	H	H	CH_3	H
AZA2	H	CH_3	CH_3	H
AZA3	H	H	H	H
AZA4	OH	H	H	H
AZA5	H	H	H	OH

Fig. 1. Chemical structure of AZA1, 2, 3, 4 and 5.

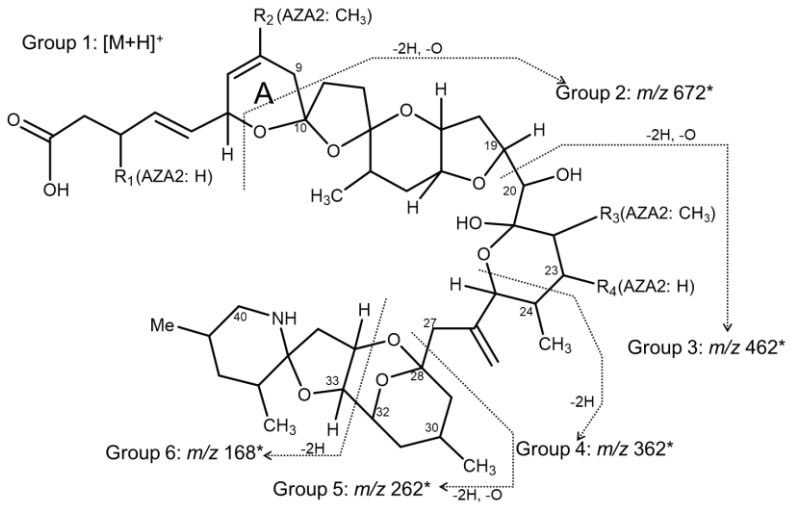

Fig. 2. The fragmentation diagram of AZAs by positive ion mode LC/MS/MS.

*Characteristic product ions in AZA2

573

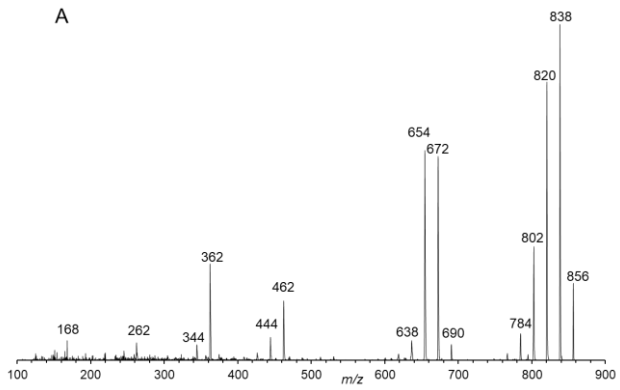
A
838
820
654
672
802
362
856
462
168
262
344
444
638
690
784
100
200
300
400
500
m/z
600
700
800
900

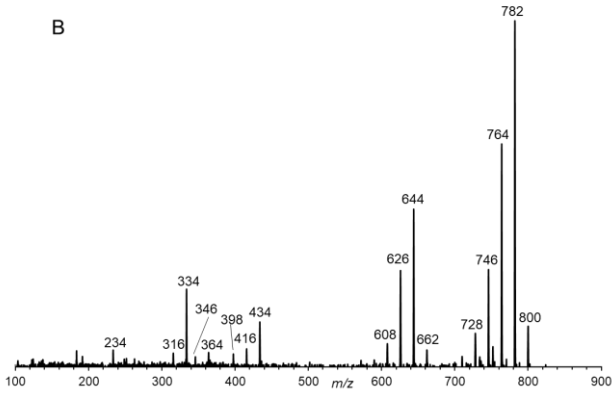
B
782
764
644
626
746
334
346
398
434
728
800
234
316
364
416
608
662
100
200
300
400
500
m/z
600
700
800
900

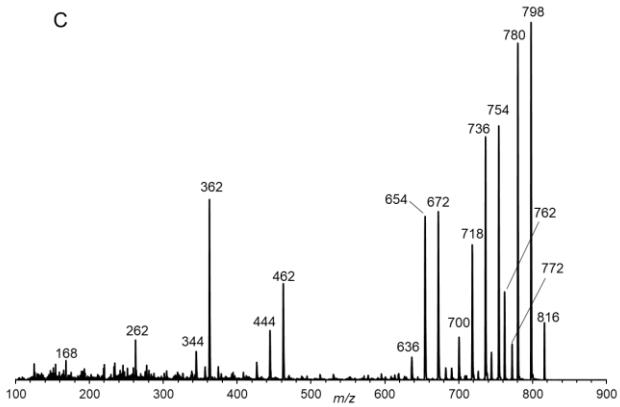
C
798
780
754
736
362
654
672
762
718
772
462
816
700
444
262
344
636
168
100
200
300
400
500
m/z
600
700
800
900

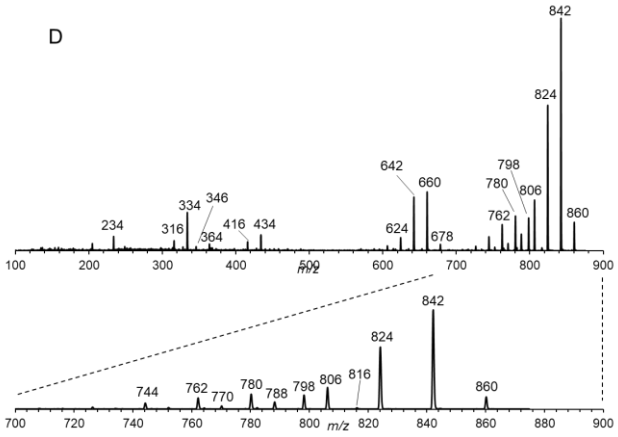

Fig. 3. Enhanced product ion LC-MS/MS spectra obtained for culture strains of *A. poporum*. (A) AZA2, (B) compound 19, (C) compound 20 and (D) compounds 21 and 22.

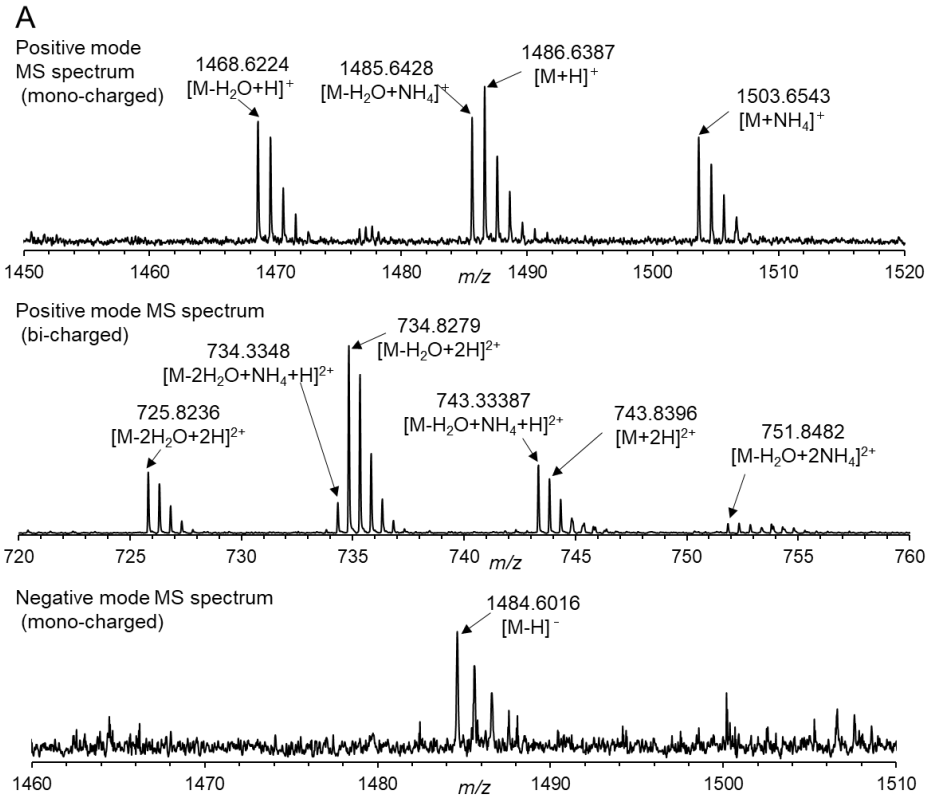

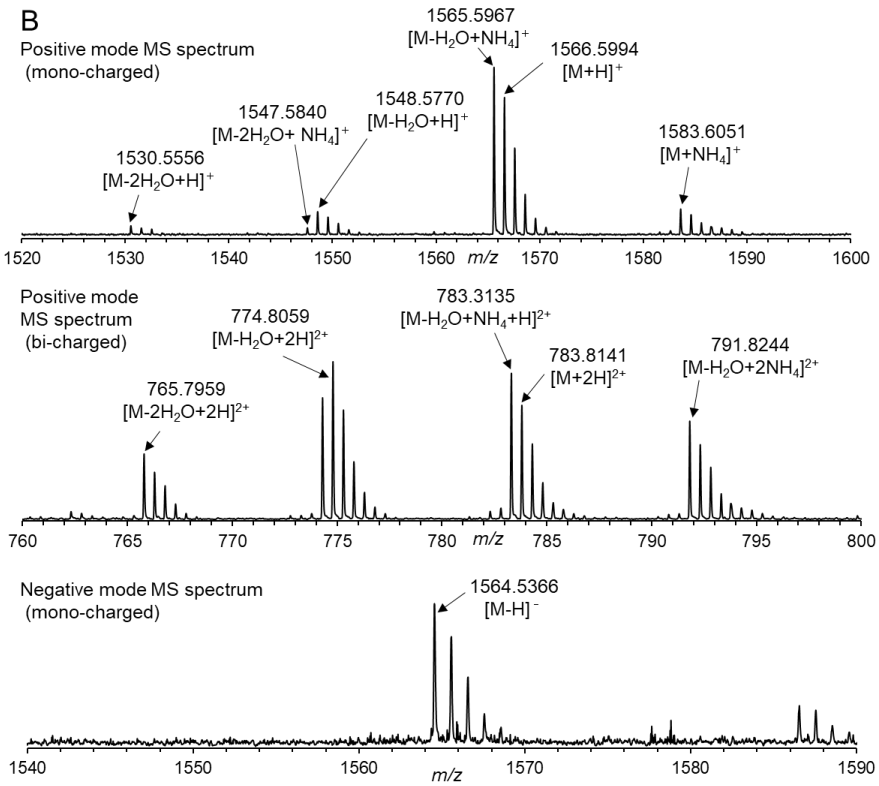
B
Positive mode MS spectrum
(mono-charged)
1565.5967
[M-H2O+NH4]+
1566.5994
[M+H]+
1547.5840
[M-2H2O+ NH4]+
1548.5770
[M-H2O+H]+
1583.6051
[M+NH4]+
1530.5556
[M-2H2O+H]+
1520
1530
1540
1550
1560
m/z
1570
1580
1590
1600
Positive mode
MS spectrum
(bi-charged)
774.8059
[M-H2O+2H]2+
783.3135
[M-H2O+NH4+H]2+
783.8141
[M+2H]2+
791.8244
[M-H2O+2NH4]2+
765.7959
[M-2H2O+2H]2+
760
765
770
775
780
m/z
785
790
795
800
Negative mode MS spectrum
(mono-charged)
1564.5366
[M-H]-
1540
1550
1560
m/z
1570
1580
1590

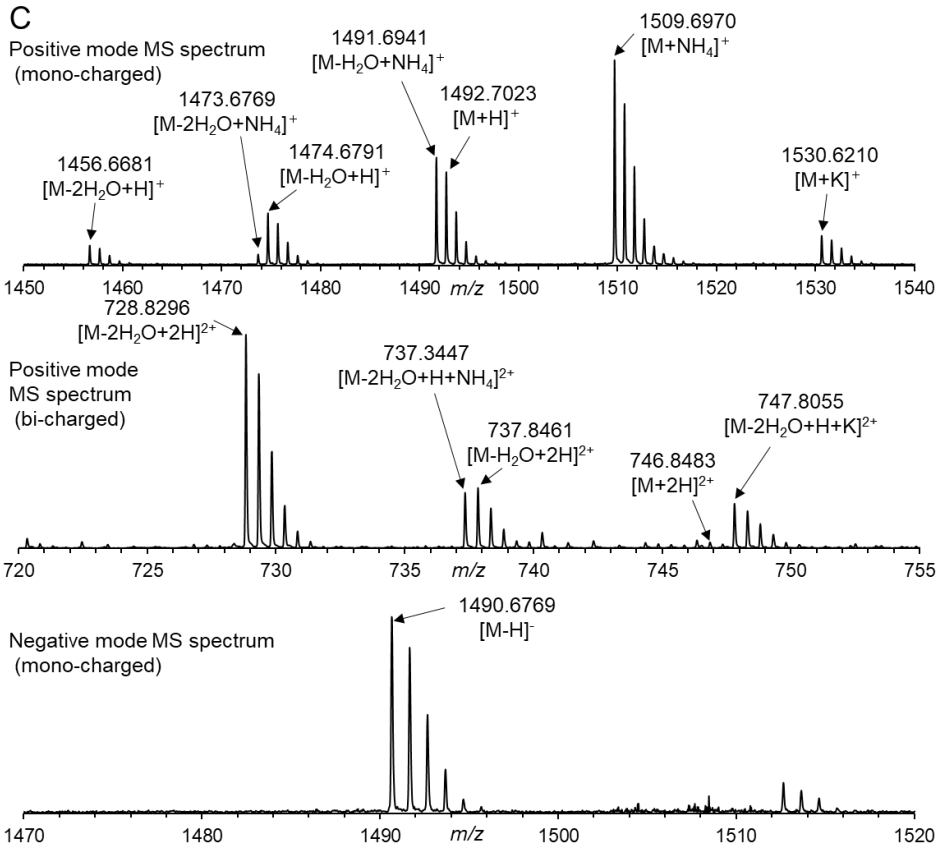
C
Positive mode MS spectrum
(mono-charged)
1456.6681
[M-2H2O+H]+
1473.6769
[M-2H2O+NH4]+
1474.6791
[M-H2O+H]+
1491.6941
[M-H2O+NH4]+
1492.7023
[M+H]+
1509.6970
[M+NH4]+
1530.6210
[M+K]+
1450 1460 1470 1480 1490 m/z 1500 1510 1520 1530 1540
Positive mode
MS spectrum
(bi-charged)
728.8296
[M-2H2O+2H]2+
737.3447
[M-2H2O+H+NH4]2+
737.8461
[M-H2O+2H]2+
746.8483
[M+2H]2+
747.8055
[M-2H2O+H+K]2+
720 725 730 735 m/z 740 745 750 755
Negative mode MS spectrum
(mono-charged)
1490.6769
[M-H]-
1470 1480 1490 m/z 1500 1510 1520

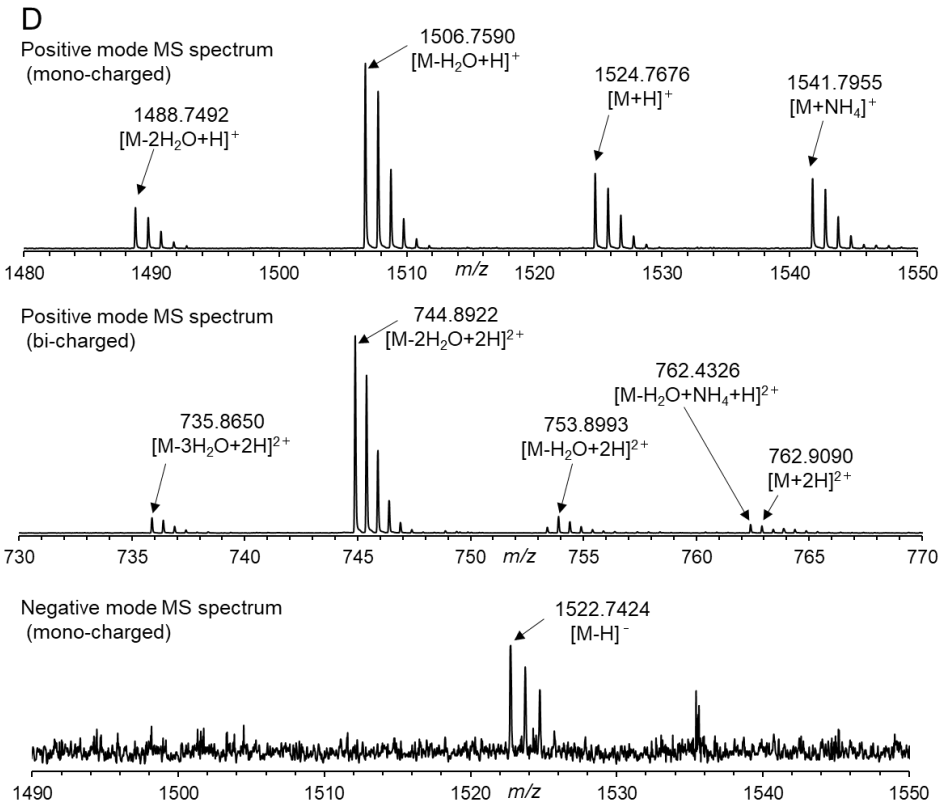
D
Positive mode MS spectrum
(mono-charged)
1506.7590
[M-H2O+H]+
1524.7676
[M+H]+
1541.7955
[M+NH4]+
1488.7492
[M-2H2O+H]+
1480 1490 1500 1510 m/z 1520 1530 1540 1550
Positive mode MS spectrum
(bi-charged)
744.8922
[M-2H2O+2H]2+
762.4326
[M-H2O+NH4+H]2+
735.8650
[M-3H2O+2H]2+
753.8993
[M-H2O+2H]2+
762.9090
[M+2H]2+
730 735 740 745 750 m/z 755 760 765 770
Negative mode MS spectrum
(mono-charged)
1522.7424
[M-H]-
1490 1500 1510 1520 m/z 1530 1540 1550

588

589

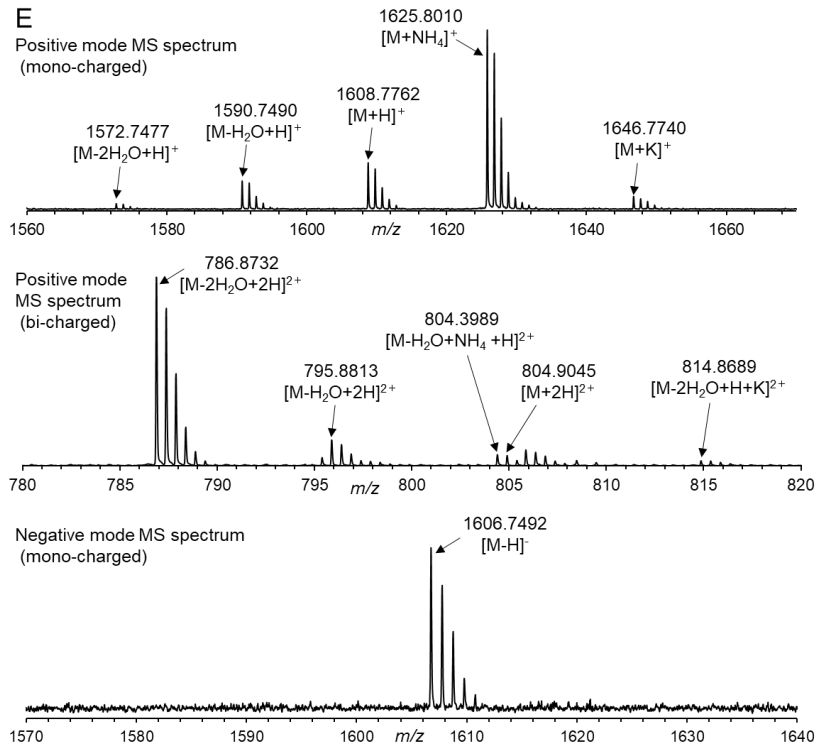
E
Positive mode MS spectrum
(mono-charged)
1625.8010
[M+NH4]+
1608.7762
[M+H]+
1590.7490
[M-H2O+H]+
1572.7477
[M-2H2O+H]+
1646.7740
[M+K]+
1560 1580 1600 m/z 1620 1640 1660
Positive mode
MS spectrum
(bi-charged)
786.8732
[M-2H2O+2H]2+
804.3989
[M-H2O+NH4 +H]2+
795.8813
[M-H2O+2H]2+
804.9045
[M+2H]2+
814.8689
[M-2H2O+H+K]2+
780 785 790 795 m/z 800 805 810 815 820
Negative mode MS spectrum
(mono-charged)
1606.7492
[M-H]-
1570 1580 1590 1600 m/z 1610 1620 1630 1640

590

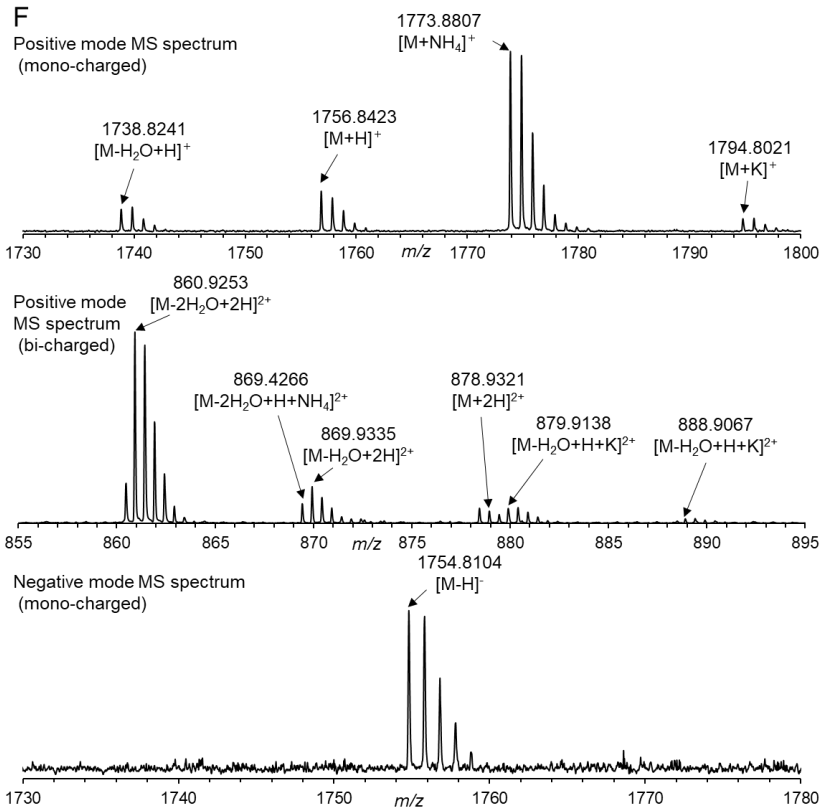

Fig. 4. MS spectra obtained for culture strains of *A. poporum* by positive ion mode and negative ion mode LC/QTOFMS. (A) compound 23, (B) compound 28, (C) compound 24, (D) compound 27, (E) compound 29 and (F) compound 30.

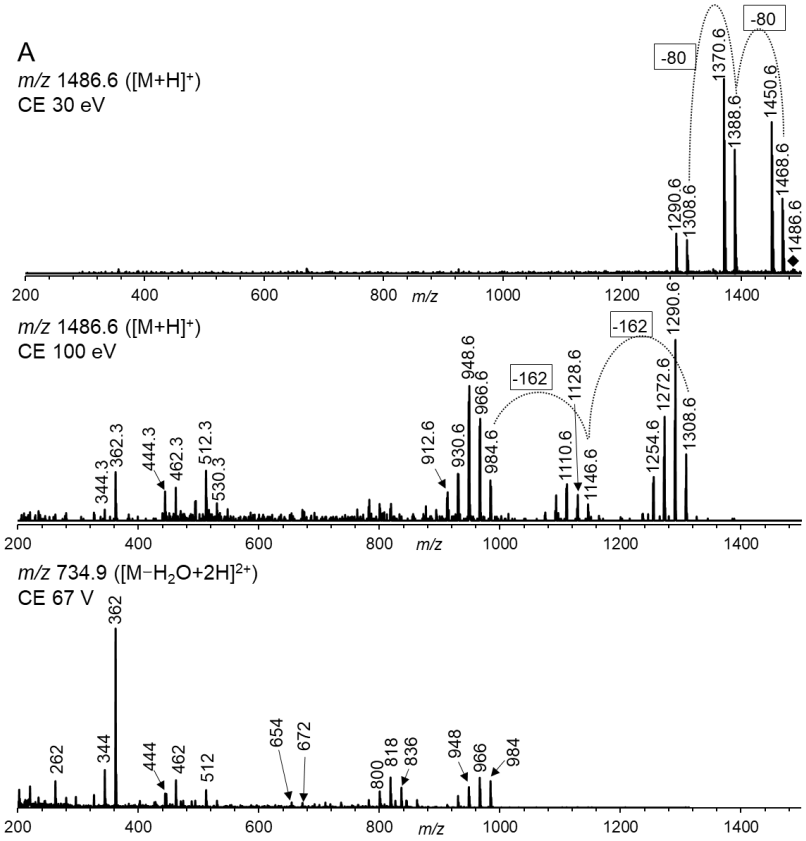
A
m/z 1486.6 ([M+H]+)
CE 30 eV
-80
-80
1290.6
1308.6
1370.6
1388.6
1450.6
1468.6
1486.6
m/z 1486.6 ([M+H]+)
CE 100 eV
-162
-162
344.3
362.3
444.3
462.3
512.3
530.3
912.6
930.6
948.6
966.6
984.6
1110.6
1128.6
1146.6
1254.6
1272.6
1290.6
1308.6
m/z 734.9 ([M−H2O+2H]2+)
CE 67 V
262
344
362
444
462
512
654
672
800
818
836
948
966
984
200
400
600
800
1000
1200
1400
m/z

596

597

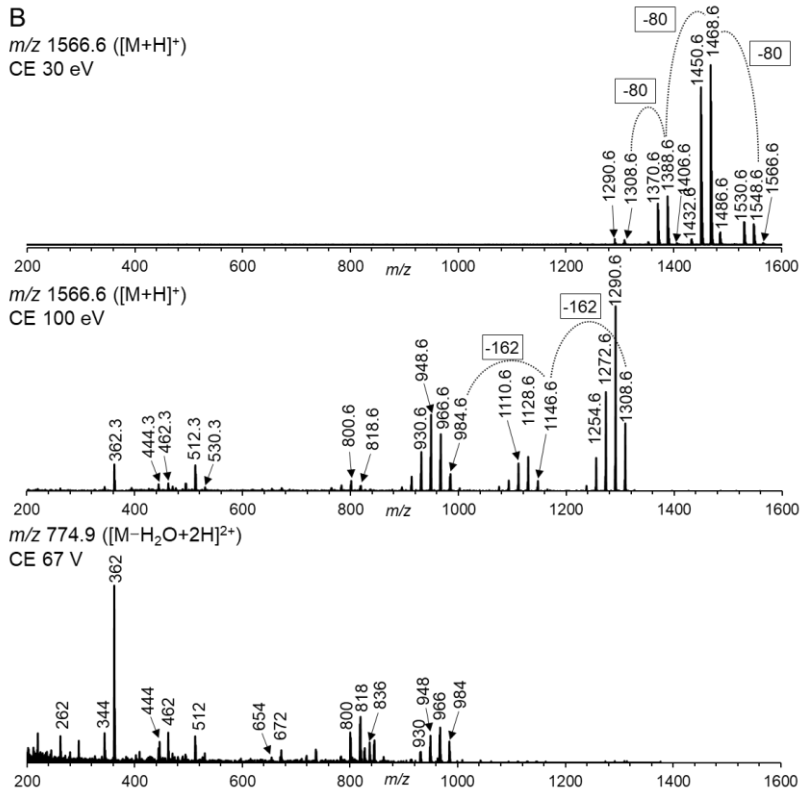
B
m/z 1566.6 ([M+H]+)
CE 30 eV
-80
-80
-80
1290.6
1308.6
1370.6
1388.6
1406.6
1432.6
1450.6
1468.6
1486.6
1530.6
1548.6
1566.6
m/z 1566.6 ([M+H]+)
CE 100 eV
-162
-162
362.3
444.3
462.3
512.3
530.3
800.6
818.6
930.6
948.6
966.6
984.6
1110.6
1128.6
1146.6
1254.6
1272.6
1290.6
1308.6
m/z 774.9 ([M−H2O+2H]2+)
CE 67 V
262
344
362
444
462
512
654
672
800
818
836
930
948
966
984
200
400
600
800
1000
1200
1400
1600
m/z

598

599

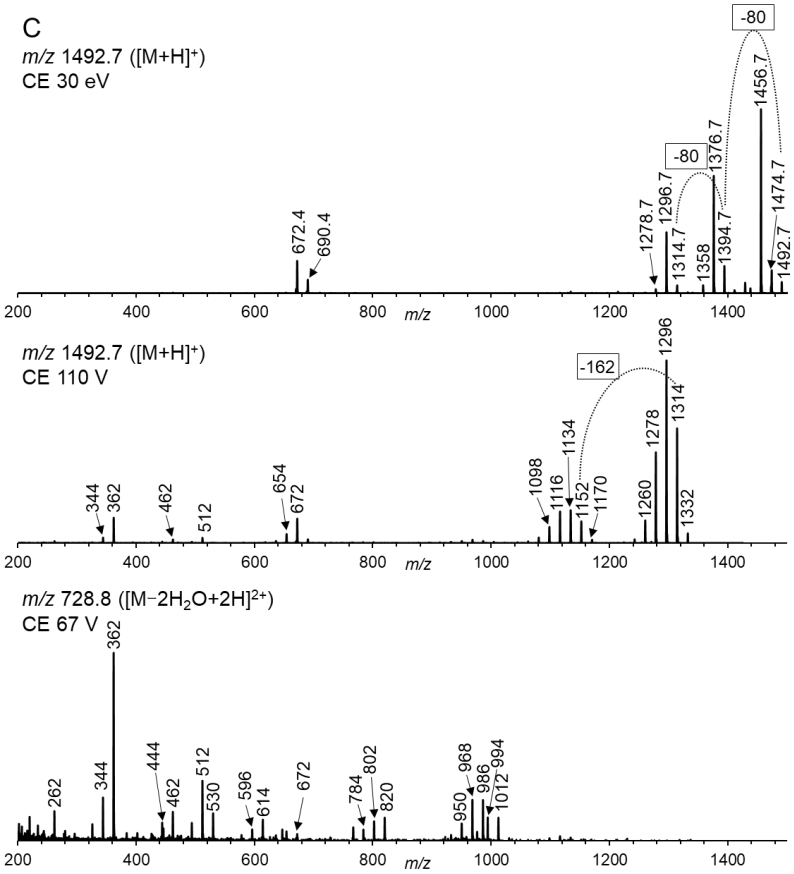
C
m/z 1492.7 ([M+H]+)
CE 30 eV
-80
-80
672.4
690.4
1278.7
1296.7
1314.7
1358
1376.7
1394.7
1456.7
1474.7
1492.7
m/z 1492.7 ([M+H]+)
CE 110 V
-162
344
362
462
512
654
672
1098
1116
1134
1152
1170
1260
1278
1296
1314
1332
m/z 728.8 ([M−2H2O+2H]2+)
CE 67 V
262
344
362
444
462
512
530
596
614
672
784
802
820
950
968
986
994
1012
200
400
600
800
1000
1200
1400
m/z

600

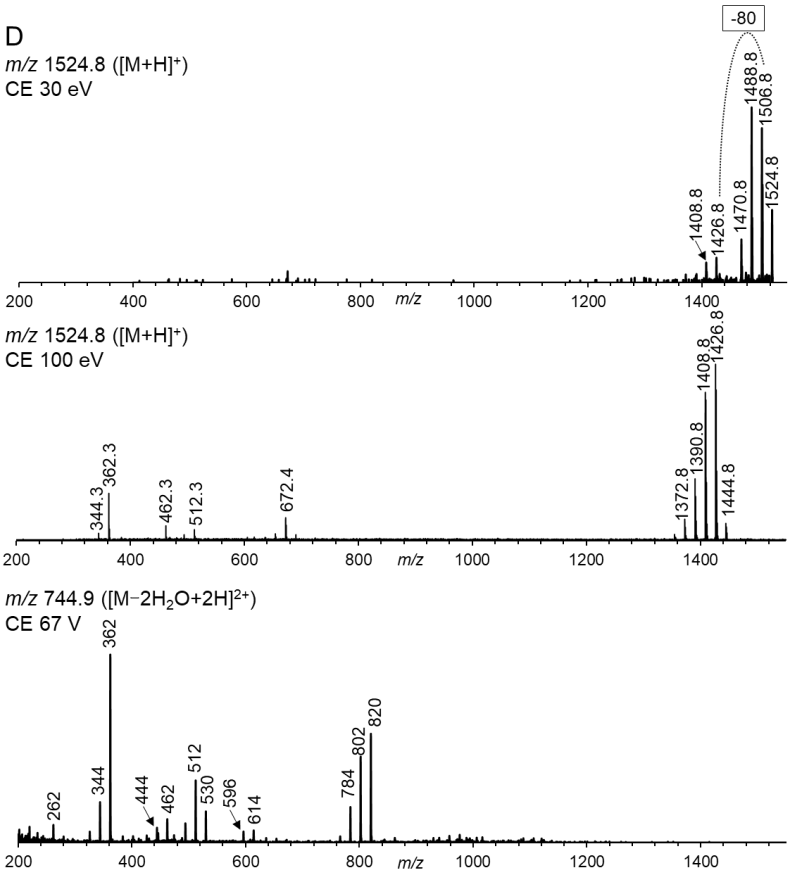
D
m/z 1524.8 ([M+H]+)
CE 30 eV
-80
1408.8
1426.8
1470.8
1488.8
1506.8
1524.8
m/z 1524.8 ([M+H]+)
CE 100 eV
344.3
362.3
462.3
512.3
672.4
1372.8
1390.8
1408.8
1426.8
1444.8
m/z 744.9 ([M−2H2O+2H]2+)
CE 67 V
262
344
362
444
462
512
530
596
614
784
802
820
m/z
200
400
600
800
1000
1200
1400

601

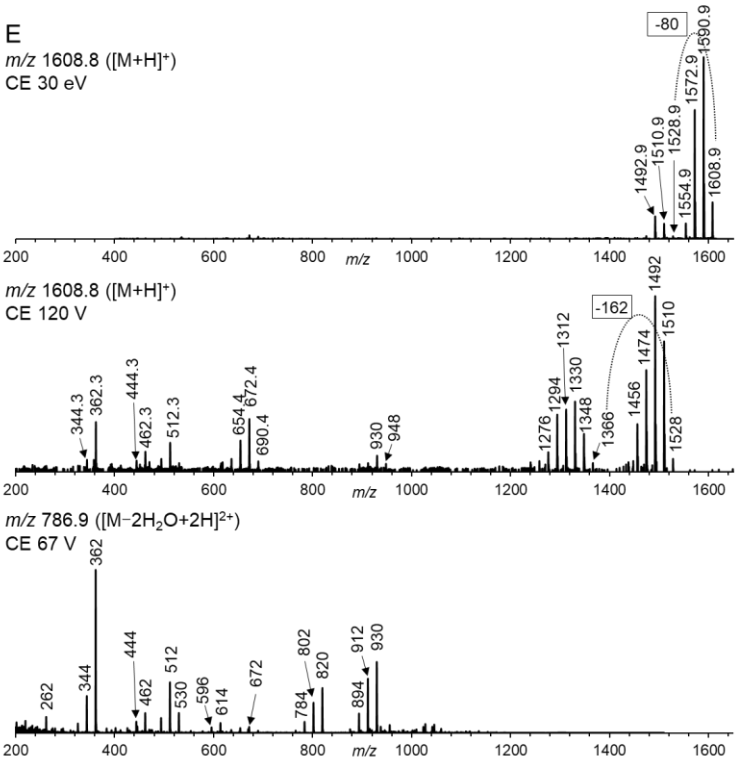
E
m/z 1608.8 ([M+H]+)
CE 30 eV
-80
1492.9
1510.9
1528.9
1554.9
1572.9
1590.9
1608.9
m/z 1608.8 ([M+H]+)
CE 120 V
-162
344.3
362.3
444.3
462.3
512.3
654.4
672.4
690.4
930
948
1276
1294
1312
1330
1348
1366
1456
1474
1492
1510
1528
m/z 786.9 ([M−2H2O+2H]2+)
CE 67 V
262
344
362
444
462
512
530
596
614
672
784
802
820
894
912
930
m/z
200
400
600
800
1000
1200
1400
1600

602

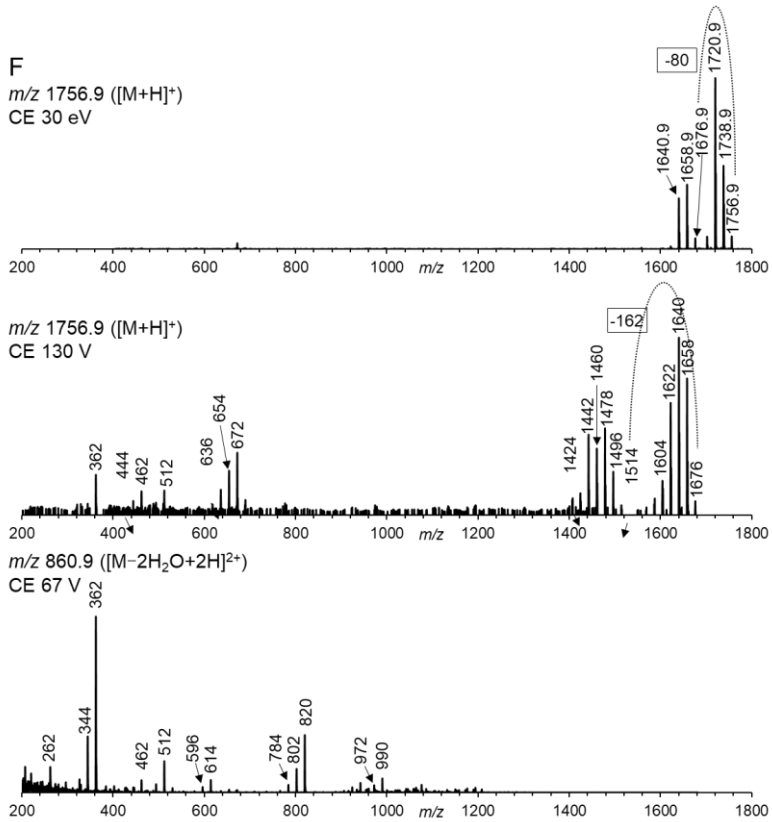

603

604 Fig. 5. MS/MS spectra obtained for culture strains of *A. poporum*. (A) compound 23,

605 (B) compound 28, (C) compound 24, (D) compound 27, (E) compound 29 and (F)

606 compound 30. Target ions and collision energies for MS/MS analyses are shown in

607 each MS/MS spectra.

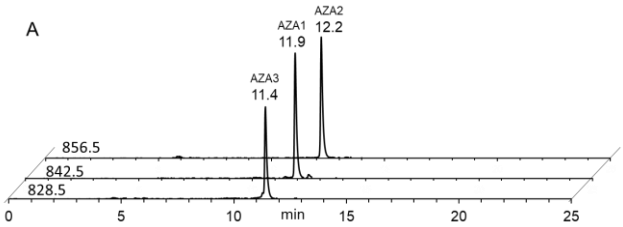

608

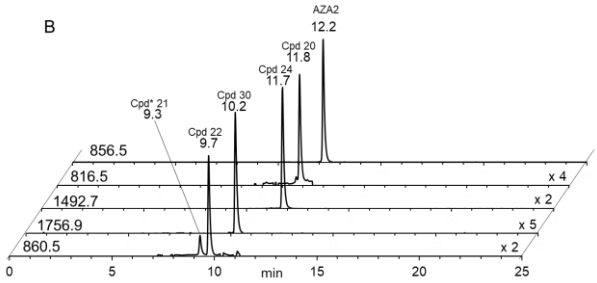

609

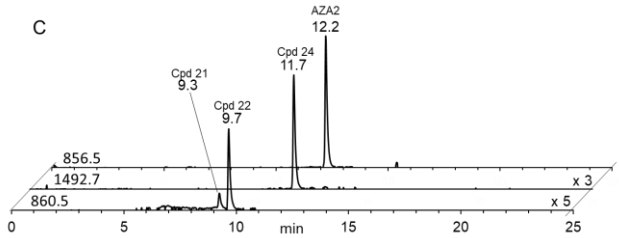

610

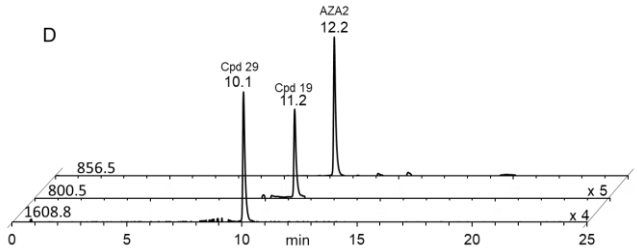

611

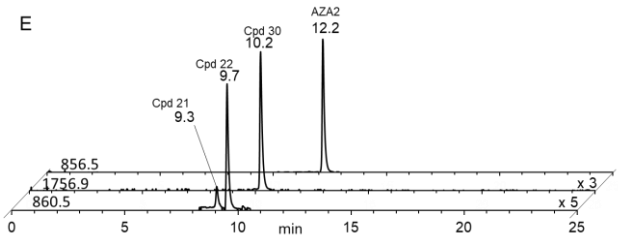

612

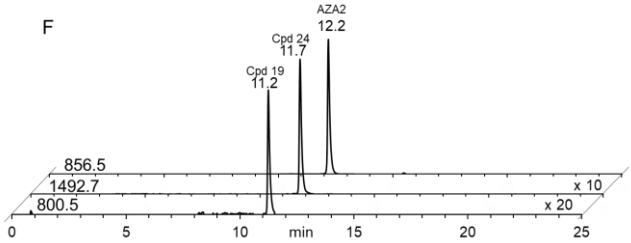

613

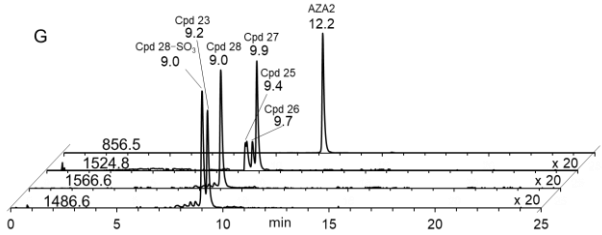

614

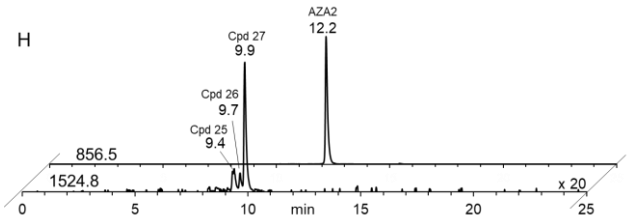

Fig. 6. Extracted ion chromatograms of AZA1, 2, 3 standard mixture and new AZAs in *A. poporum* strains on the LC-QTOFMS with a C8 column. Identification and retention time are shown at the top of the peak. (A) AZA1, 2, 3 standard mixture, (B) strain MoAz592, (C) strain MoAz593, (D) strain MoAz594, (E) strain LAM125, (F) strain TOY121, (G) strain mdd421 and (H) strain HM536

Table 1 SRM ion channels of AZAs including new AZA analogues detected in our present study.

SRM transition			AZAs	CE (V)
708.4	>	362.3	Compound 1	73
716.4	>	362.3	AZA33	73
800.4	>	348.3	AZA53	73
810.4	>	362.3	AZA25	73
816.4	>	348.3	AZA39	73
816.4	>	362.3	AZA34	73
824.4	>	362.3	AZA26, AZA27	73
826.4	>	362.3	AZA48, AZA60	73
828.4	>	360.3	AZA43	73
828.4	>	362.3	AZA3, AZA58	73
830.4	>	348.3	AZA38, AZA52	73
830.4	>	362.3	AZA35	73
832.4	>	364.3	Compound 6	73
838.4	>	362.3	AZA28	73
840.4	>	362.3	AZA49, AZA61	73
842.4	>	348.3	AZA40, AZA50	73
842.4	>	362.3	AZA1, AZA6, AZA29	73
844.4	>	362.3	AZA4, AZA5, AZA57	73
846.4	>	348.3	AZA37	73
854.4	>	360.3	AZA41	73
856.4	>	362.3	AZA2, AZA30, AZA31	73
858.4	>	348.3	AZA36, AZA51	73
858.4	>	362.3	AZA7, AZA8, AZA9, AZA10	73
858.4	>	364.3	Compound 8	73
860.4	>	362.3	AZA59	73
868.4	>	360.3	AZA55	73
870.4	>	360.3	AZA42	73
870.4	>	362.3	AZA32, AZA54, AZA62	73
872.4	>	362.3	AZA11, AZA12, AZA13, AZA17, Compounds 5, 11, 13	73
872.4	>	378.3	Compounds 10, 12	73
874.4	>	362.3	AZA14, AZA15, Compounds 2, 3, 4, 9	73
884.4	>	362.3	AZA56	73
886.4	>	362.3	AZA18, AZA19	73
888.4	>	362.3	AZA16, AZA21, AZA44	73
900.4	>	362.3	AZA20	73
902.4	>	362.3	AZA22, AZA23, AZA45	73
904.4	>	362.3	AZA46	73
916.4	>	362.3	AZA24	73
918.4	>	362.3	AZA47	73
918.4	>	362.3	AZA2 phosphate ester-H_2O	73
936.4	>	362.3	AZA2 phosphate ester	73
800.4	>	334.3	compound 19	73
816.4	>	362.3	compound 20	73
860.4	>	334.3	compounds 21, 22	73
1290.6	>	362.3	compounds 23, 28	100
1296.8	>	362.3	compound 24	110
1408.8	>	362.3	compounds 25, 26, 27	100
1510.8	>	362.3	compound 29	120
1640.9	>	362.3	compound 30	130

625 The channels below the dotted line were set for new AZAs discovered in our present

626 study.

627

Table 2 The measured accurate mass of $[M+H]^+$, elemental compositions, and retention times obtained for AZA analogues using LC-QTOFMS.

Compounds	$[M+H]^+$ *m/z*	MS/MS fragment ions Group2	Group3	Group4	Group5	Error (ppm)	Elemental compositions	Relative reteintion time Hypersil C8	ADME	Detections Precursor ion scan	Neutral ion scan	Identifications	Strains
1	708.4311	—	462	362	262	0.9	$C_{38}H_{61}NO_{11}$	0.72	0.69	✓	✓	AZA2-10C12HO	mdd421, HM536, MoAz592[*2], MoAz593, MoAz594, TOY121, LAM125
7	872.5123	672	462	362	262	-5.9	$C_{48}H_{73}NO_{13}$	0.89	0.86	✓	✓	AZA11	mdd421, HM536, MoAz594
8	858.5271	674	464	364	264	4.7	$C_{48}H_{75}NO_{12}$	0.91	0.88	✓	✓	AZA2+2H	mdd421, HM536, TOY121
9	874.5286	672	462	362	262	-4.9	$C_{48}H_{75}NO_{13}$	0.90	0.88	✓	✓	AZA2+2HO	mdd421, HM536, MoAz592, MoAz594, LAM125
12	872.5126	688	478	378	278	2.5	$C_{48}H_{73}NO_{13}$	0.98	0.97	✓	✓	AZA11 isomer	mdd421, MoAz594, LAM125
17	856.5181	672	462	362	262	1.3	$C_{48}H_{73}NO_{12}$	1.00	1.00	✓	✓	AZA2	mdd421, HM536, MoAz592, MoAz593, MoAz594, TOY121, LAM125
19[*1]	800.4925	644	434	334	234	2.2	$C_{45}H_{69}NO_{11}$	0.92	0.90	ND	✓	AZA2-3C4HO	MoAz594, TOY121
20	816.4895	672	462	362	262	-0.2	$C_{45}H_{69}NO_{12}$	0.95	0.94	✓	✓	AZA2-3C4H	MoAz592, MoAz594
21	860.4734	660	434	334	234	6.6	$C_{46}H_{69}NO_{14}$	0.78	0.69	ND	✓	AZA2-2C4H+2O	MoAz592, MoAz593, LAM125
22	860.4752	660	434	334	234	4.5	$C_{46}H_{69}NO_{14}$	0.77	0.73	ND	✓	AZA2-2C4H+2O	MoAz592, MoAz593, LAM125
23	1486.6387	672	462	362	262	—	—	0.75	0.63	✓	ND	—	mdd421
24	1492.7023	672	462	362	262	—	—	0.93	0.85	✓	ND	—	MoAz592, MoAz593, TOY121
25	1524.7659	672	462	362	262	—	—	0.76	0.65	✓	ND	—	mdd421, HM536
26	1524.7571	672	462	362	262	—	—	0.79	0.68	✓	ND	—	mdd421, HM536
27	1524.7818	672	462	362	262	—	—	0.80	0.70	✓	ND	—	mdd421, HM536
28	1566.5994	672	462	362	262	—	—	0.73	0.60	✓	ND	—	mdd421
29	1608.7998	672	462	362	262	—	—	0.82	0.71	✓	ND	—	MoAz594
30	1756.8638	672	462	362	262	—	—	0.83	0.72	✓	ND	—	MoAz592, LAM125

[*1] Underlined numbers; putative novel AZA analogues

[*2] Underlined strains; new strains analyzed in our present study

Table 3 Elemental compositions of key MS/MS product ions detected from *A. poporum* strains by LC/QTOFMS.

Compounds	MS/MS Fragment ions Group1 *m/z*	Error (ppm)	Elemental compositions	Group2 *m/z*	Error (ppm)	Elemental compositions	Group3 *m/z*	Error (ppm)	Elemental compositions	Group4 *m/z*	Error (ppm)	Elemental compositions	Group5 *m/z*	Error (ppm)	Elemental compositions
AZA2 standard	856.5201	0.5	$C_{48}H_{74}NO_{12}$	672.4100	0.9	$C_{38}H_{58}NO_9$	462.3214	0.1	$C_{27}H_{44}NO_5$	362.2686	1.1	$C_{22}H_{36}NO_3$	262.1797	1.6	$C_{16}H_{24}NO_2$
17	856.5181	2.9	$C_{48}H_{74}NO_{12}$	672.4102	0.7	$C_{38}H_{58}NO_9$	462.3203	1.6	$C_{27}H_{44}NO_5$	362.2684	1.6	$C_{22}H_{36}NO_3$	262.1806	1.7	$C_{16}H_{24}NO_2$
19	800.4900	5.5	$C_{45}H_{70}NO_{11}$	644.3778	2.3	$C_{36}H_{54}NO_9$	434.2888	3.1	$C_{25}H_{40}NO_5$	334.2367	3.0	$C_{20}H_{32}NO_3$	234.1482	2.9	$C_{14}H_{20}NO_2$
20	816.4810	10.1	$C_{45}H_{70}NO_{12}$	672.4087	2.7	$C_{38}H_{58}NO_9$	462.3223	-2.0	$C_{27}H_{44}NO_5$	362.2681	2.3	$C_{22}H_{36}NO_3$	262.1792	3.8	$C_{16}H_{24}NO_2$
21	860.4691	11.6	$C_{46}H_{70}NO_{14}$	660.3699	6.4	$C_{36}H_{54}NO_{10}$	434.2856	10.3	$C_{25}H_{40}NO_5$	334.2360	11.0	$C_{20}H_{32}NO_3$	234.1467	9.2	$C_{14}H_{20}NO_2$
22	860.4730	7.1	$C_{46}H_{70}NO_{14}$	660.3724	2.8	$C_{36}H_{54}NO_{10}$	434.2848	12.3	$C_{25}H_{40}NO_5$	334.2354	6.7	$C_{20}H_{32}NO_3$	234.1481	3.2	$C_{14}H_{20}NO_2$
23	1486.6387	—	—	672.4121	-2.2	$C_{38}H_{58}NO_9$	462.3211	0.7	$C_{27}H_{44}NO_5$	362.2697	-2.1	$C_{22}H_{36}NO_3$	262.1797	-5.9	$C_{16}H_{24}NO_2$
24	1492.7023	—	—	672.4112	-0.9	$C_{38}H_{58}NO_9$	462.3220	-1.3	$C_{27}H_{44}NO_5$	362.2690	-0.2	$C_{22}H_{36}NO_3$	262.1799	1.0	$C_{16}H_{24}NO_2$
25 (26[*1], 27[*1])	1524.7659	—	—	672.4042	9.5	$C_{38}H_{58}NO_9$	462.3152	13.3	$C_{27}H_{44}NO_5$	362.2690	12.5	$C_{22}H_{36}NO_3$		—	
28	1566.5994	—	—	672.4056	6.1	$C_{38}H_{58}NO_9$	462.3175	8.5	$C_{27}H_{44}NO_5$	262.2691	-0.5	$C_{22}H_{36}NO_3$		—	
29	1608.7998	—	—	672.4107	-0.2	$C_{38}H_{58}NO_9$	462.3212	0.6	$C_{27}H_{44}NO_5$	362.2682	2.0	$C_{22}H_{36}NO_3$	262.1794	3.0	$C_{16}H_{24}NO_2$
30	1756.8638	—	—	672.4060	6.9	$C_{38}H_{58}NO_9$	462.3185	6.3	$C_{27}H_{44}NO_5$	362.2666	6.6	$C_{22}H_{36}NO_3$	262.1777	9.5	$C_{16}H_{24}NO_2$

[*1] Elemental compositions of key MS/MS product ions of compounds 26 and 27 were not obtained due to minute amounts.

Table 4 The measured accurate mass differences of product ions detected by MS/MS analysis using LC-QTOFMS.

		Compound 23		Compond 24		Compound 25	Compound 28			Compound 29	Compound 30	AZA2 phosphate
		m/z 1468.6–*m/z* 1388.6	*m/z* 1388.6–*m/z* 1308.7	*m/z* 1456.7–*m/z* 1376.7	*m/z* 1376.7–*m/z* 1296.7	*m/z* 1506.7–*m/z* 1426.8	*m/z* 1548.6–*m/z* 14568.6	*m/z* 1468.6–*m/z* 1388.6	*m/z* 1388.6–*m/z* 1308.7	*m/z* 1590.8–*m/z* 1492.8	*m/z* 1738.8–*m/z* 1658.8	*m/z* 900.0–*m/z* 820.5
#1		79.9578	79.9546	79.9578	79.9590	79.9492	79.9499	79.9528	79.9543	79.9552	79.9523	79.965862
#2		79.9606	79.9402	79.9534	79.9578	79.9481	79.9538	79.9528	79.9550	79.9525	79.9509	79.966514
#3		79.9586	79.9531	79.9556	79.9590	79.9547	79.9544	79.9521	79.9566	79.9554	79.9536	79.964509
Average (n=3)		79.9590	79.9493	79.9556	79.9586	79.9507	79.9527	79.9525	79.9553	79.9544	79.9523	79.9656
RSD (%)		0.0015	0.0081	0.0023	0.0007	0.0036	0.0025	0.0004	0.0012	0.0016	0.0014	0.0010
err value*	$-HPO_3$	-6.80	-16.47	-10.20	-7.22	-15.11	-13.06	-13.24	-10.45	-11.42	-13.52	-0.15
(10^{-3} *m/z* units)	$-SO_3$	2.71	-6.95	-0.68	2.30	-5.59	-3.55	-3.73	-0.93	-1.91	-4.01	9.36

*Actual value (average)－Theoretical value

Table 5 The peak area percentages of AZAs in *A. poporum* strains obtained by LC-MS/MS SRM analysis and LC-QTOFMS survey scan analysis.

			Peak area (%)													
Compounds	$[M+H]^+$	Identifications	mdd421 (ribotype C1)		HM536 (ribotype C1)		MoAz592 (ribotype A2)		MoAz593 (ribotype A2)		MoAz594 (ribotype A2)		LAM125 (ribotype A2)		TOY121 (ribotype A2)	
			SRM	QTOF	SRM	QTOF	SRM	QTOF	SRM	QTOF	SRM	QTOF	SRM	QTOF	SRM	QTOF
1	708.4	AZA2-10C12HO	0.2	1.6	2.0	1.5	1.3	1.9	4.9	6.4	1.6	0.2	3.1	2.7	1.0	1.4
2	874.5	AZA2+2HO	0.1	0.0	1.0	0.1	ND	ND	ND	ND	ND	ND	ND	ND	ND	ND
3	874.5	AZA2+2HO	0.5	0.1	1.6	0.5	ND	ND	ND	ND	ND	ND	ND	ND	ND	ND
4	874.5	AZA2+2HO	ND	ND	0.2	0.0	ND	ND	ND	ND	ND	ND	ND	ND	ND	ND
5	872.5	AZA11 isomer	0.2	0.1	0.2	0.3	ND	ND	ND	ND	ND	ND	ND	ND	ND	ND
6	832.5	AZA2-2C	ND	ND	1.7	1.1	ND	ND	ND	ND	ND	ND	ND	ND	ND	ND
7	872.5	AZA11	0.4	0.1	0.2	0.2	ND	ND	ND	ND	0.9	0.9	0.1	0.0	ND	ND
8	858.5	AZA+2H	0.3	0.9	3.9	0.8	ND	ND	ND	ND	ND	ND	ND	ND	1.4	0.7
9	874.5	AZA2+2HO	0.4	0.6	0.8	1.2	0.6	0.9	ND	ND	0.6	0.4	0.7	0.0	ND	ND
10	872.5	AZA11 isomer	0.0	ND	ND	ND	ND	ND	ND	ND	ND	ND	ND	ND	ND	ND
11	872.5	AZA11 isomer	0.2	0.3	0.1	0.1	ND	ND	ND	ND	ND	ND	ND	ND	ND	ND
12	872.5	AZA11 isomer	0.1	0.3	ND	ND	ND	ND	2.1	2.3	0.3	0.3	1.3	2.7	ND	ND
13	872.5	AZA11 isomer	0.3	1.3	0.2	0.5	ND	ND	ND	ND	ND	ND	ND	ND	ND	ND
14	830.5	AZA35	ND	ND	2.6	6.9	ND	ND	ND	ND	ND	ND	ND	ND	ND	ND
15	936.5	AZA2 phosphate	5.0	12.1	4.8	5.2	ND	ND	ND	ND	ND	ND	ND	ND	ND	ND
16	918.5	AZA2 phosphate ester-2HO	0.1	1.0	ND	ND	ND	ND	ND	ND	ND	ND	ND	ND	ND	ND
17	856.5	AZA2	71.2	68.3	69.1	58.8	89.7	82.4	65.2	70.8	85.1	82.7	71.4	68.1	83.6	90.1
18	870.5	AZA2 methl ester	4.2	1.8	4.4	5.1	ND	ND	ND	ND	ND	ND	ND	ND	ND	ND
19	800.5	AZA2-3C4HO	ND	ND	ND	ND	0.6	0.9	1.6	1.9	1.2	1.3	ND	ND	3.6	4.2
20	816.5	AZA2-3C4H	ND	ND	ND	ND	2.8	3.2	ND	ND	2.0	1.6	ND	ND	ND	ND
21	860.5	AZA2-2C4H+2O	ND	ND	ND	ND	1.0	1.4	1.6	1.5	1.5	1.8	4.4	5.1	ND	ND
22	860.5	AZA2-2C4H+2O	ND	ND	ND	ND	3.3	6.3	5.9	9.3	5.6	6.4	18.7	19.9	ND	ND
23	1486.6	—	1.4	1.0	ND	ND	ND	ND	ND	ND	ND	ND	ND	ND	ND	ND
24	1492.7	—	ND	ND	ND	ND	ND	ND	18.6	7.9	ND	ND	ND	ND	10.4	3.7
25	1524.8	—	0.3	0.6	1.6	5.0	ND	ND	ND	ND	ND	ND	ND	ND	ND	ND
26	1524.8	—	0.3	0.5	1.4	3.4	ND	ND	ND	ND	ND	ND	ND	ND	ND	ND
27	1524.8	—	0.8	1.7	4.2	9.4	ND	ND	ND	ND	ND	ND	ND	ND	ND	ND
28	1566.6	—	13.9	7.7	ND	ND	ND	ND	ND	ND	ND	ND	ND	ND	ND	ND
29	1608.8	—	ND	ND	ND	ND	ND	ND	ND	ND	1.3	4.3	ND	ND	ND	ND
30	1756.9	—	ND	ND	ND	ND	0.7	2.9	ND	ND	ND	ND	0.3	1.6	ND	ND

Table S1 ESI conditions of various analysis mode by LC-QTOMS.

	Positive ion mode survey scan	Negative ion mode survey scan	Positive ion mode MS/MS
Capillary voltage (v)	4500	3500	4500
Dry heater (°C)	180	180	200
Dry gas flow (L/min)	10	8	10
Nebulizer gas (Bar)	1.6	1.6	1.6
Collision cell RF (Vpp)	650	150	300
Collision Energy (eV)	10	10	10
Transfer time (μs)	120	70	80
Pre pulse storage time (μs)	10	5	8
Mass range	*m/z* 400−*m/z* 2000	*m/z* 400−*m/z* 3000	*m/z* 50−*m/z* 2000

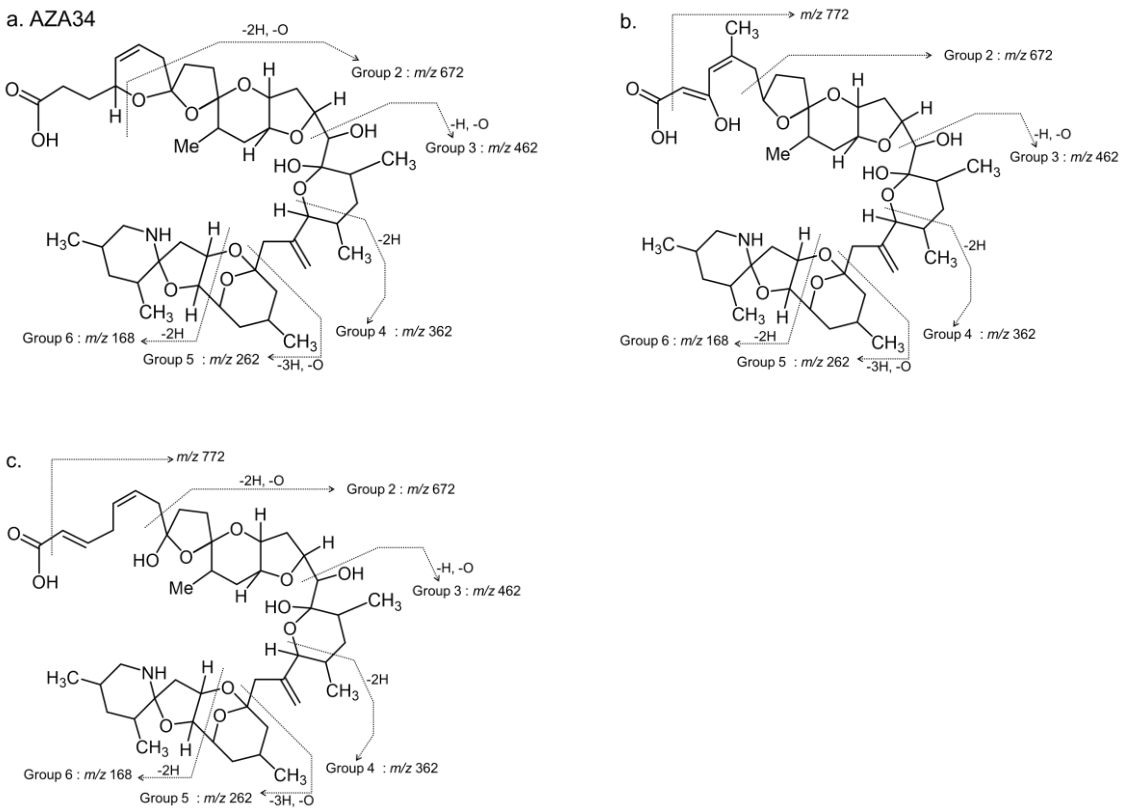

Fig. S1 (a) The chemical structures of AZA34 [15] and (b, c) the two putative structures of compound 20.